Research Article | Vol. 29, No. 15 / 19 July 2021 / Optics Express 23487
Optics EXPRESS

Optimization of selective laser etching (SLE) for glass micromechanical structure fabrication

AGNĖ BUTKUTĖ,[1,*] TOMAS BARAVYKAS,[2] JOKŪBAS STANČIKAS,[1,2] TITAS TIČKŪNAS,[2] ROKAS VARGALIS,[2] DOMAS PAIPULAS,[1] VALDAS SIRUTKAITIS,[1] AND LINAS JONUŠAUSKAS[1,2]

[1]*Laser Research Center, Vilnius University, Saulėtekio Ave. 10, Vilnius LT- 10223, Lithuania*
[2]*Femtika Ltd., Saulėtekio Ave. 15, Vilnius LT- 10224, Lithuania*
[*]*agne.butkute@ff.vu.lt*

Abstract: In this work, we show how femtosecond (fs) laser-based selective glass etching (SLE) can be used to expand capabilities in fabricating 3D structures out of a single piece of glass. First, an investigation of the etching process is performed, taking into account various laser parameters and scanning strategies. These results provide critical insights into the optimization of the process allowing to increase manufacturing throughput. Afterward, various complex 3D glass structures such as microfluidic elements embedded inside the volume of glass or channel systems with integrated functional elements are produced. A single helix spring of 1 mm diameter is also made, showing the possibility to compress it by 50%. Finally, 3D structuring capabilities are used to produce an assembly-free movable ball-joint-based chain and magnet-actuated Geneva mechanism. Due to minimized friction caused by low (down to 200 nm RMS) surface roughness of SLE-produced structures, the Geneva mechanism was shown to be capable of rotating up to 2000 RPM.

1. Introduction

Over the years glass was proven to be material of choice in a multitude of rapidly developing science: microfluidics [1–3], micromechanics [4,5] and microoptics [6]. The reason for such popularity lies in the superb mechanical properties of the material, alongside it being completely transparent in the visible and near-infrared (IR) and chemically inert in organic solvents. As a result, there is a substantial drive to produce various functional microdevices out of this material. True 3D mesoscale structures are especially interesting. In essence, mesoscale objects combine overall size in practically usable mm-cm range with functionality enabled by the nano-/microfeatures. Various glass processing techniques exist. However, most of them are complicated and/or unable to produce 3D structures in mesoscale. Direct laser ablation [7] is a simple solution or , but it lacks the 3D aspect. Direct 3D printing has been shown as a tool to make 3D objects, yet the resolution is then limited to tens-hundreds of μm [8,9]. Stereolithography and subsequent heat treatment is another option, but then the resolution is still in the range of μm [10]. Due to the rapid development of light structural polymers [11], a similar operation can be performed employing two-photon polymerization (2PP/TPP) based 3D laser lithography (3DLL) [12]. However, the necessity for highly specialized monomer resins and complex post-processing remains. Therefore, all these methods have some severe drawbacks if straightforward glass 3D meso-fabrication is in question.

The most promising technology to produce 3D mesoscale glass structures is SLE [13,14]. The technology is based on selectively modifying transparent medium *via* femtosecond (fs) laser radiation which is becoming a more and more widespread tool for material processing [15]. During ultrashort pulses exposure, modifications of type II (i.e. nanogratings) are formed in the volume of the material [16]. Subsequently, the exposed sample is submerged in the etchant (such

#430623 https://doi.org/10.1364/OE.430623
Journal © 2021 Received 3 May 2021; revised 20 Jun 2021; accepted 25 Jun 2021; published 9 Jul 2021

Optics EXPRESS

as potassium hydroxide (KOH) or hydrofluoric acid (HF)). Then, modified regions dissolve up to ~ thousand times faster than surrounding medium [17]. The ratio between the etching rate of unmodified and modified regions is called selectivity. SLE allows true 3D glass manufacturing [2,18]. Potentially, many types of glasses and crystals such as fused silica [13], borosilicate [19,20], crystalline sapphire [21–23] or Yttrium aluminum garnet (YAG) [24] can be processed in this manner. However, so far this process is not exploited widely. The problem lies in the complex nature of light-matter interaction and difficulties in optimizing the technique for true 3D fabrication, sparking various works aimed at improving this aspect of the technique [25,26].

Due to the 3D capability of SLE, one of the main parameters to consider is selectivity. It is influenced by both SLE process steps. On one hand, selectivity depends on a created material modification which is governed by scanning peculiarities and laser parameters. Selectivity is also highly affected by etchant [17] and etching properties [27]. In practice, various etchants such as HF [19,28] and KOH [1,29,30] can be used. However, it has been already demonstrated that KOH allows obtaining higher selectivity than etching with HF [17]. The process dependency on various laser and scanning parameters such as pulse energy [19,29], pulse duration [29,30], polarization [16], pulse repetition rate [31] or even scanning velocity [3,29] and scanning spacing [17] were already reported to some extent. However, most of these studies were done for single-line (1D) channels and are lacking a 3D aspect. To fully understand these nuances, the selectivity of different 2D planes out of which complex arbitrary 3D structures can be constructed have to be understood. Furthermore, selectivity dictates that to acquire complex shapes the geometry of the structure should be altered to account for the dissolving of unmodified regions. Thus, overall, while the premise of SLE is simple, so far realization was proven to be rather complicated.

This work aims to optimize SLE 3D structure fabrication. We will concentrate on optimizing laser exposure and scanning parameters as these can be easily tuned using standard laser systems. We will begin by exploring the optimal laser and scanning parameters for 2D plane formation alongside streamlining the whole exposure algorithm. All of this is shown to simplify and accelerate the processing. Proposed methods are then employed to manufacture complex assembly-free microfluidic and micromechanical structures. These include embedded microfluidic channels with integrated micro mechanical elements, ball joint-like structure, high compression spring, and Geneva mechanism. All of these structures are evaluated qualitatively and quantitatively showing that improved fabrication techniques do not compromise the quality or functionality of the structures. The acquired results are shown in the broader perspective, relating it to previous SLE works, additive manufacturing, and potential application areas.

2. Materials and methods

In this work, we used almost pure amorphous SiO_2 which is normally referred to as fused silica (UVFS). "Laser Nanofactory" setup (Femtika Ltd.) was used in this work [32]. "Pharos" laser (Light Conversion Ltd.) is used as a radiation source. Radiation parameters: 1030 nm wavelength, pulse duration ~ 700 fs, pulse repetition rate - 610 kHz. The laser beam is focused on the sample with a 20x 0.45 NA objective with automated aberrations correction. That means, aberration compensation depends on the writing depth in the glass. Thus, aberrations are compensated for all modifications written in described experiments. For all modifications written in XY plane focusing depth was 500 μm. Spot size: 1.5 μm diameter focused beam spot in XY direction and ~15 μm in the Z direction. For sample positioning, Aerotech positioning stages and Galvano scanners are used. After the sample is exposed to fs laser, the modified volume is etched out in 10 mol/l concentration KOH solution at 90°C. Samples were characterized using various optical microscopes and scanning electron microscopes (SEM). The surface roughness was measured using an atomic force microscope (AFM).

Optics EXPRESS

3. Results

3.1. Optimization of manufacturing process

Through the years SLE processing peculiarities were investigated in numerous articles. However, to fully comprehend the process of 3D object manufacturing, the link between translation velocity, polarization, and structuring direction in relation to the etching direction has to be understood. This study was started by performing a set of experiments related to this topic. First, a 1D experiment was performed, the general schematics of this test are given in Fig. 1(a). By translating the sample in XY direction single lines were written inside the volume of the glass with particular sets of parameters such as different pulse energies, scanning velocities, and polarisation. Afterward, the selectivity tests of the planes (i.e. 2D case) were performed. A set of lines with particular spacing in XY or Z direction were written inside the glass according to the schemes shown in Fig. 2. Despite the varying spacing between lines, the width of the line blocks for hatching tests and the depth of the line blocks for the slicing test were kept the same (40 μm). Next, the substrates of the glass were cut in the middle according to the markings on the scheme. Sample cutting was needed only in those cases when modifications were completely inside the volume of glass and have no exit to any surface. Samples were subsequently immersed into the etchant for 1 hour, then rinsed into distilled water and dried in ambient air. Finally, the length of the etched channels was measured by using an optical microscope. This way 1D experiment showed selectivity dependence on the pulse energy, writing velocity, and light polarization. Meanwhile, 2D experiments showed plane selectivity dependence on the overlapping of scanned lines, pulse energy, light polarization, and etching direction.

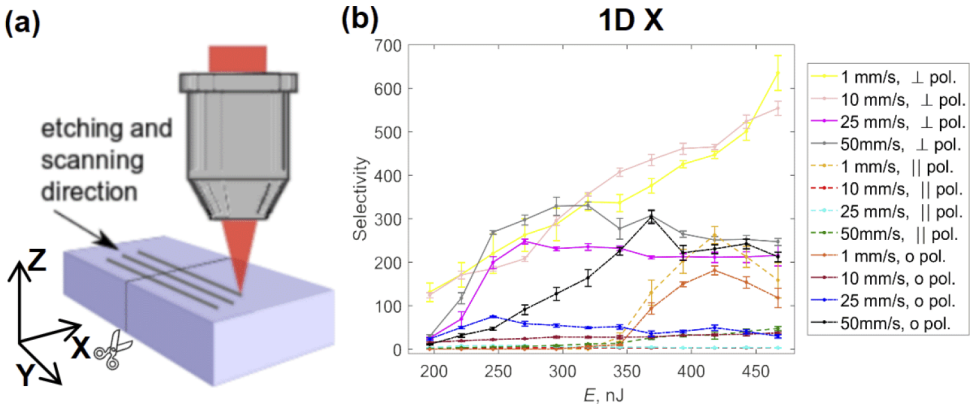

Fig. 1. (a) Schematics of 1D selectivity experiment. (b) Single line selectivity test results. Single lines are written in XY plane with various parameters such as different pulse energies, scanning velocities, and light polarization.

The results of 1D experiments are shown in Fig. 1. After writing single lines in the XY plane the highest obtained selectivity value is around ~650. It was observed with the polarization perpendicular to the scanning direction, the lowest tested scanning velocity (1 mm/s), and the highest tested pulse energy (492 nJ). Particular scanning velocity and pulse repetition rate combination control overlapping between pulses which define thermal relaxation of the energy. Overall, the femtosecond pulse duration is too short to transfer the energy to the lattice of the material, thus processing can be called "cold" [33]. However, if pulse spatial and temporal overlapping is high, volume heats. On the other hand, overlapping of the pulses change and the total dose absorbed by volume unit. Thus, with lower scanning velocity we transfer more energy to the material and observe stronger thermal effects which leads to greater volume modification, changes modification morphology [19] and gives higher selectivity. Also, it can be

Optics EXPRESS

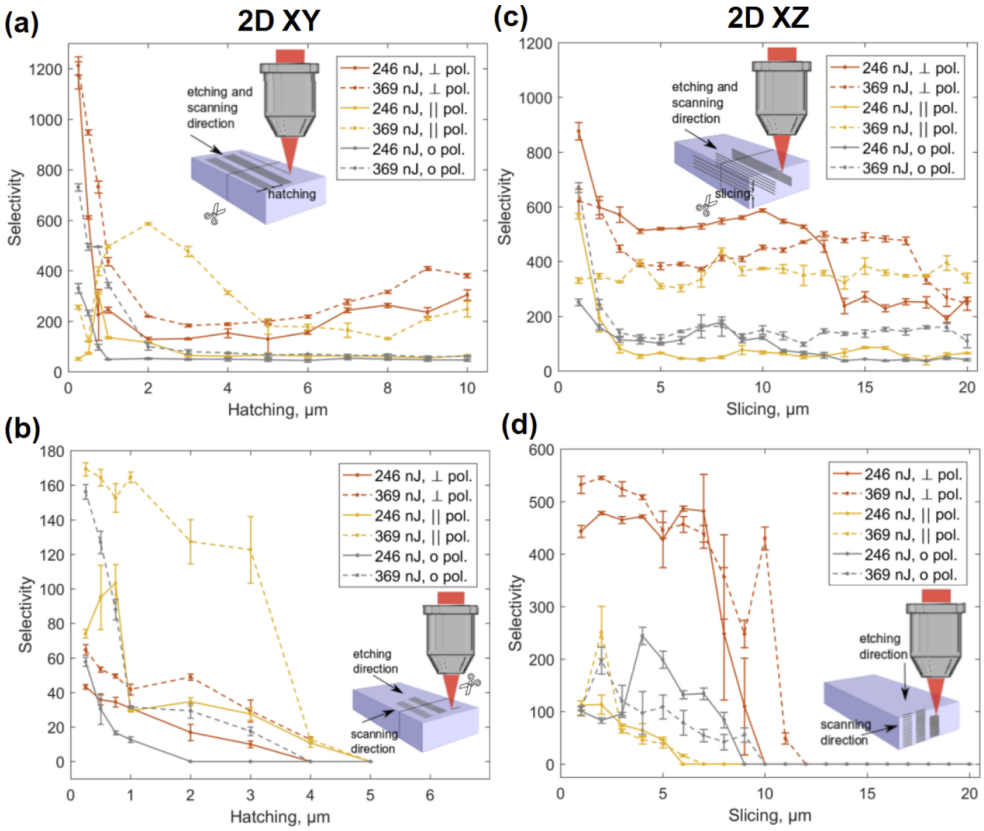

Fig. 2. 2D (plane) selectivity test results. (a) XY plane etched parallel to the scanning direction selectivity dependency to hatching, (b) XY planes etched perpendicularly to the scanning direction selectivity dependency to hatching, (c) XZ planes etched parallel to the scanning direction selectivity dependency to slicing, (d) XZ planes etched perpendicular to the scanning direction selectivity dependency to slicing.

seen that polarization perpendicular to the scanning direction gives the highest selectivity value. Meanwhile, polarization parallel to the scanning direction shows the lowest selectivity. Thus, these etching process dependency on polarization have been already reported in previous works [16] and in this work obtained results correlates with previously reported results. Furthermore, the selectivity has a tendency to saturate for the most tested parameters. Interestingly, the selectivity even starts to drop when the pulse energy is increased. This was also demonstrated in previous works [19,29]. However, the absolute value of pulse energy depends on the whole parameter set. Thus, optimal pulse energy values need to be chosen for the most effective SLE process.

As the goal of this work was to optimize processing for high-throughput 3D glass manufacturing, several important conclusions were drawn from acquired results. The highest tested translation velocity (50 mm/s) was chosen for further experiments in order to get the highest throughput. Also, we choose 2 pulse energies - the lowest possible pulse energy which gives selectivity value close to the maximum in case of polarization perpendicular to the scanning direction (246 nJ), and pulses energy value which gives the highest value with circular polarization (369 nJ). Higher pulse energy is not a practical choice for complex 3D structure fabrication due to high volume tensions which lead to cracks in the structure. Usually, the lowest possible pulse energy

Optics EXPRESS

is beneficial because lower pulse energy leads to lower tensile stress in the volume minimizing the possibility of cracks formation.

While 1D experiments give interesting insights into the process, it does not paint the full picture. 2D experiments are a lot closer to the real experimental conditions of 3D fabrication and, thus, are investigated next. The motivation underlying such experiments lies in a rather limited understanding of the etching process outside single-line fabrication (i.e. 1D case). It is known that light polarization effects nanogratings orientation direction [16]. In the case of polarization perpendicular to the scanning direction, pores parallel to the scanned lines are obtained. When considering it in the context of SLE, this configuration of the nanogratings allows for the etchant to penetrate deep inside the modification. In this way of light polarization parallel to the scanning direction, pores perpendicular to the scanning direction are obtained. With this nanogratings configuration etchant easily penetrates only to the first pore, resulting in a thin wall between pores that need to be etched. These thin walls between the pores slow down the etching. However, these insights are viable when considering single lines. The process becomes more complex when we form the planes of multiple lines. Different polarization-induced modifications might be induced in the same volume of the material, potentially overlapping each other [34]. Additionally, in the case of planes, the initial opening formed during etching is bigger, allowing easier diffusion of etched glass, further expediting the process. It has been already reported some planes such as XZ plane etching properties, however, due to the voxel shape, this does not represent the full picture of the process for 3D structure formation. Thus, here we present a broader picture of 2D plane research which leads to a better understanding of arbitrary shape structure formation.

The primary goal of 2D experiments was to test etching rate peculiarities depending on the direction of the inscribed plane and etching direction. The ultra-fast laser can be used to fabricate free-form 3D shapes without the usage of slicing and hatching, for instance, microlenses can be made as continuous spirals [35]. However, such cases are rare and the most common, practical, and simplest way to 3D fabricate structures is simply slicing and hatching. Thus, for this discussion, we will only consider orthogonal planes tied to axes of the positioning system: XY, XZ, and YZ. From a laser structuring perspective, XZ and YZ planes can be considered to be equivalent, as in Gaussian focusing case voxel is symmetrical in XY plane, leaving only two types of planes: horizontal and vertical. From the etching experiment side, one additional variable is etching direction, i.e. from which side inscribed modifications will be exposed to the etchant. Therefore, 4 distinct cases need to be tested to get the full picture of the process [Fig. 2].

2D horizontal (XY) plane test results when etching directions are parallel and perpendicular to the scanning directions are shown in Figs. 2(a) and 2(b) respectively. When the etching direction is parallel to the line writing direction, the highest selectivity of around 1200 is obtained by inscribing lines with the lowest tested hatching step (0.25 μm) and also by adopting polarization perpendicular to the scanning direction. In our experiment, by increasing hatching values to more than 2 μm the overlapping between adjacent lines is lost (spot diameter of used 0.45 NA objective - $2\omega_0$ = 1.5 μm) and selectivity drops to the values below 500. It is remarkably similar to the single-line selectivity achieved in 1D experiments. As expected, when the etching direction is perpendicular to the scanning direction maximum the obtained selectivity is around 6 times lower than in the previous case test (up to ~17). However, this test determines the maximum possible hatching step, which in this case is 4 μm. From the practical perspective, during structuring, both cases are combined (if XZ and YZ planes are fabricated without tuning polarization), leading to undesired results, as if selectivity is close to 0 for at least one direction it will be impossible to etch the entire 3D structure. As an outcome, fast polarization control is needed if light polarization is to be tied to the translation direction. As a realization of such an approach is hard to achieve, a lot simpler solution is to use circular polarization. Then, translation direction is no more a variable during structuring. Additionally, as shown in this work, the etching rate does not drop

Optics EXPRESS

dramatically when circular polarization is used. Thus, due to practical considerations, circular polarization was used to fabricate all the 3D structures shown in this work.

Later, vertical 2D (XZ/YZ) plane tests were performed. The results of these tests are shown in Figs. 2(c) and 2(d). The highest selectivity is achieved with the lowest tested slicing between scanning lines (1 μm). When slicing is increased selectivity drops drastically. However, when polarization is parallel to the scanning direction, a further increment in slicing starts to slightly increase the etching rate. This indicates that interference between modifications creates suitable volume nanopatterns which affect the etching properties. The test with the etching direction perpendicular to the scanning direction determines the maximum possible slicing parameter which is around 10 μm and higher slicing values will be an obstacle for surface etching. Overall, the higher maximal slicing step can be explained by the already mentioned inherent elongation of the voxel in the Z direction due to Gaussian focusing properties. Here we find out that with our tested setup maximum hatching could be 4 μm and slicing 10 μm. Nonetheless, for the practical 3D structure formation lower values are desired to have higher selectivity.

Finally, it was decided to measure the surface roughness of the etched surfaces. Here we measured both XY and XZ/YZ surfaces roughness. These results are depicted in Figs. 3(a) and 3(b). In both plane cases, the lowest surface roughness of around 200 nm RMS is obtained with the lowest tested slicing/hatching (0.5 μm). By increasing the spacing between lines, the roughness value rises together and reaches around 800 nm RMS. Looking back to the same surface selectivity, it can be concluded that higher surface selectivity gives lower surface roughness. Selectivity correlation with surface roughness has been already reported in other works [27]. However, polarization influence on fabricated structure surface roughness was not studied before. As shown before polarization strongly affects selectivity. Nonetheless, obtained surface roughness dependency on polarization is not very significant and the lowest value in both cases is obtained independent of polarization. In conclusion spacing between scanning lines affects formed surfaces more significantly than pulse energy or light polarization. Also, in addition to minimal surface roughness, SLE allows achieving minimal taper on vertical surfaces [Fig. 3(c)]. This is very attractive for usage in precise microfluidics or as an extremely rigid molding master for soft lithography [36].

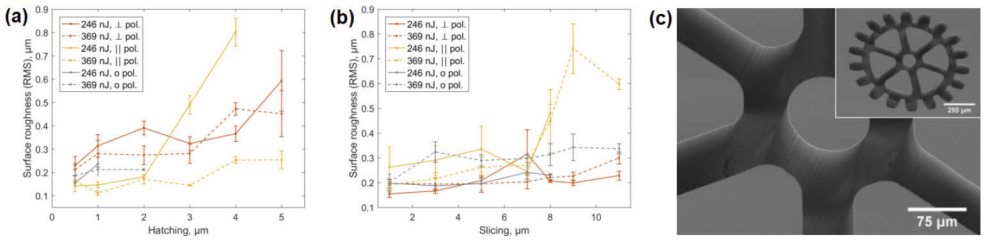

Fig. 3. Surface roughness (calculated as RMS) acquired using SLE of horizontal (a) and vertical (b) surfaces. All values are below 1 μm. (c) - Zoomed in SEM image of surfaces of an example structure (with the whole element being in the inset), showing good surface quality and minimal taper achievable in practice.

In the case of 3D structure formation scanning strategies is also a factor that should not be overlooked. Intuitively, when producing a 3D structure, it would seem that the most convenient and simplest way to fabricate the required shape would be to modify and then etch out all the unnecessary volume. That means all volume should be scanned out line by line with fixed slicing and hatching between each line and by maintaining voxel overlapping. This strategy is illustrated in Fig. 4(a). However, it is an extremely slow approach. Additionally, it might result in cracks, which appear due to excessive internal stress caused by volume overexposure. Both of these difficulties can be tackled by employing the strategy of segment scanning. Then,

Optics EXPRESS

only the contours of the structure are exposed to the laser light, while the rest of the material is divided into smaller pieces. This scanning strategy is shown in Fig. 4(b). In this way, all inscribed structures are combined out of contours and surfaces which should be scanned out by maintaining the same voxel overlapping. This strategy allows saving lots of fabrication time. For instance, dividing the standard structure into cubes with dimensions of 50 μm x 50 μm x 50 μm allows reducing fabrication time by the factor of 7. If 100 μm x 100 μm x 100 μm cubes are used manufacturing is around 14 times faster and by dividing into 200 μm x 200 μm x 200 μm cubes - around 28 faster. There is another option to scan out only the contours of the structure. This option is demonstrated in Fig. 4(c). This approach is useful for 2D structure fabrication and would allow saving even more fabrication time than dividing material into the cube.

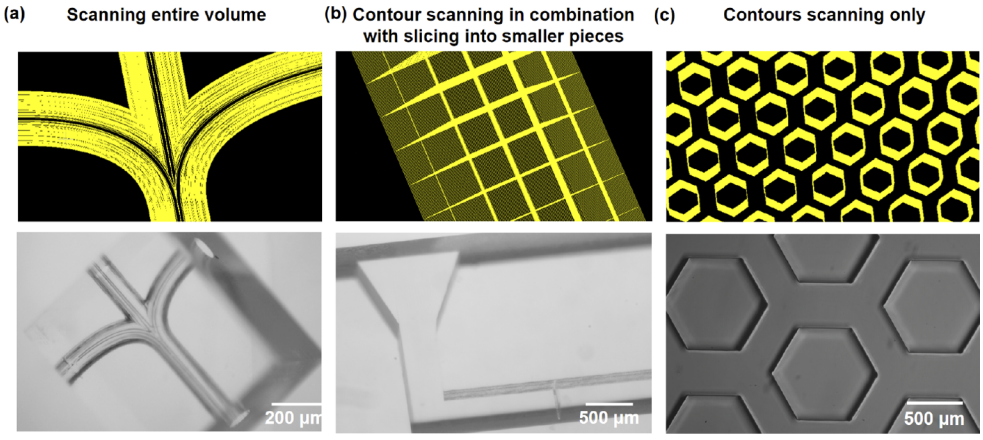

Fig. 4. Demonstration of how different scanning strategies can be applied in various structures formation. (a) Scanning entire volume used for closed channel fabrication, (b) contour scanning in combination with slicing into smaller pieces applied in open channel chip fabrication, (c) contours scanning only applied in the production of hexagon-shaped hole manufacturing.

Another advantage is that by minimizing the number of scanned lines we reduce volume tensions. The downside of this approach is the necessity to make such features at the top of the sample, as otherwise non-etched segments could not fall out. This limits the usage of such an approach in embedded structure fabrication. Additionally, segmenting prolongs etching time. It is a result of etchant needing to reach underneath produced segments. In consequence, a taper of modifications might increase, as unaffected material is also being continuously etched. For complex shape and long channel systems most of the time it is useful to scan all the volume needed to be etched. These two strategies can also be mixed together, with rougher parts of the system being segments, and more fine details being exposed in full. Thus, the scanning strategy needs to be chosen carefully for each structure individually in order to get the best compromise between the highest throughput and quality.

3.2. Fabricated 3D glass structures

There are multiple fields that could benefit from high-precision 3D mesoscale glass structure fabrication. One of the most promising applications for SLE is microfluidics. As shown in this work, SLE-made channels can have a relatively low surface roughness (~200 nm RMS). At the same time, the throughput of the technology, if the whole volume needs to be exposed, is relatively low. In contrast, laser-ablated glass channels usually will have worse surface roughness and are produced faster [37], without the need for an etching technological step. Nevertheless, SLE greatly exceeds ablation in terms of flexibility and allows to produce 3D free-form structures,

Optics EXPRESS

such as channels with integrated functional elements, or 3D channel systems embedded inside the volume of glass, as shown in Figs. 5(a) and 5(b), bringing new capabilities and flexibility to the field. These properties give a possibility to avoid other supplementary processes such as sealing of ablated channels or the necessity to use other manufacturing techniques for integration of some more trivial structures. To demonstrate what can be integrated, we created a microfluidic system with integrated deformable cantilever Figs. 5(c) and 5(d). Thin glass cantilevers are extremely simple yet potent structures that have a lot of usages [38]. In the case of cantilevers integrated into microfuildical channels, such a device was demonstrated to possibly perform a task of a very precise flow meter [39]. The main difference and improvement from the example given in the literature that SLE allows to fabricate such cantilever structure in relatively simpler manner. While normally glass is perceived as a hard material, in size range bellow ~100 μm glass can be deformed without breaking [40]. Therefore, produced 250 μm x 200 μm x 25 μm dimension cantilever could be bent using probe up to ~30 μm without breaking it.

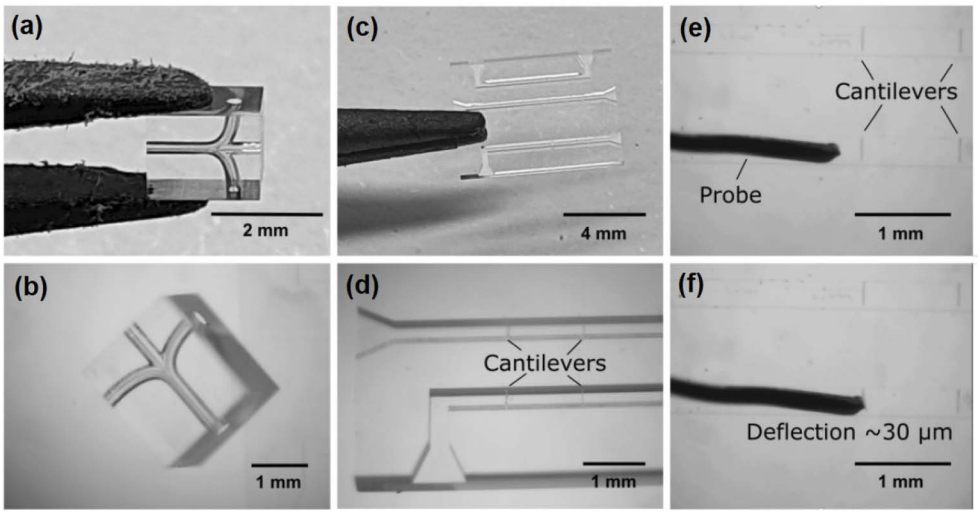

Fig. 5. Examples of various 3D microfluidic structures produced applying SLE. (a) and (b) - embedded channel sections. As such systems are in the volume of glass no sealing step is required. Furthermore, due to very low (down to ~200 nm surface roughness such systems are basically transparent. (c) and (d) - a channel system housing integrated 250 μm x 200 μm x 25 μm cantilevers. Channel cross-section - 300 μm x 300 μm. (e) and (f) shows bending of the cantilever using a hard probe. Possible deflection - up to ~30 μm.

Continuing on the topic of deformable glass structures, a single helix 4 turn spring was produced out of glass [Fig. 6(a)]. The diameter of the structure is 1 mm, with the width of the helix itself being 50 μm. The combined length of the whole helix was around 12 mm. As a result, this allowed to repeatedly compress the spring up to 50% (from 600 μm to 300 μm) without damaging it. The fabrication of such structure employed both segmenting (in the middle of the structure) and full volume exposure (for fine springs). Due to it, such a structure can be produced in ~4 min. Such springs, as they can be mass-produced on-demand in mass-customized series, could prove to be attractive in such fields as the watch industry. While not trivial at the first sight, but such structures can be made to be mechanically resistant to compressive forces and at the same time robust against shock, due to the possibility of using some advanced architectures like gyroids in the support part of the spring (which in our case is a simple bulk plate). Combined with a very small weight, such structures could be proven to be extremely mechanically resilient

Optics EXPRESS

to shock and vibrations, at the same time surpassing polymer-made micromcehanics [32] of the same type in terms of chemical and thermal resilience.

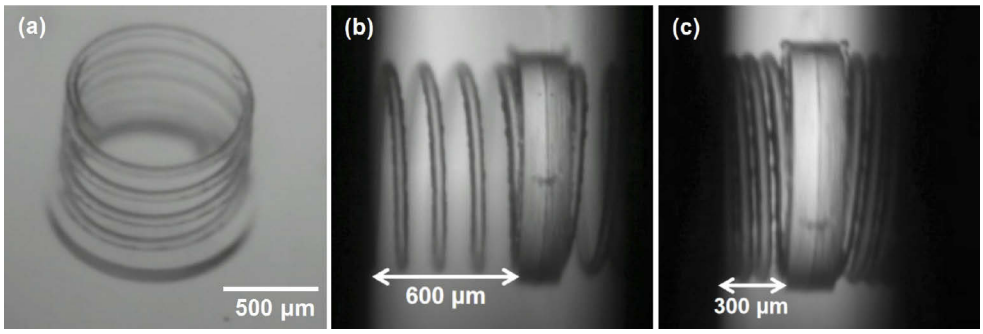

Fig. 6. Images of fused silica single helix 4 turn spring. (a) - overall view. (b) and (c) shows compression of the spring. Due to the small thickness (diameter - 50 μm) and relatively long length of the helix (12 mm) it can be compressed repeatedly from 600 to 300 μm (50% of overall helix height) without any damage to the structure.

Alternatively from deformable micromechanics, one might consider structures made out of different independently moving components. Normally, such systems are made part by part and then assembled. However, SLE allows true 3D modification of glass volume. As a result, openings needed for structure motion can be embedded before etching and then revealed by it. Therefore, assembly-free movable multi-part 3D glass structures can be produced, relatively easily, expanding current capabilities of the field of micro-mechanics. To demonstrate it, we first produced a chain with free movable ball joints. This structure employing the idea of etching out the narrow gaps between the separate parts of the structure. In this way, we create a joint-like structure that is able to move. The exact model and optical microscope photos of the manufactured structure are shown in Fig. 7. The bending amplitude of the produced structure (which is 30°) coincides well with the value predicted from the mechanical CAD model. As the structure is very complex, and the opening of the outer ball is 450 μm in diameter, the whole inside of the outer ball was exposed to the laser radiation. For this reason, the fabrication of such a structure heavily relies on the understanding of etching rates. If chosen processing parameters would be insufficient, the fine opening would either not etch out, or etch out too much, resulting in disassembly of the ball joint. Therefore, when manufacturing such fine structures substantial attention should be paid to both process and model optimization, in order to achieve the best possible result.

Finally, we fabricated a complex micromechanical structure called the Geneva mechanism [Fig. 8]. This structure contains two intermeshing elements. By rotating one gear every 360° rotation it moves and another gear by fixed 90° increments. SLE technology allows fabricating such mechanisms out of a single piece of glass without the need for an assembly step. As this structure is assembly-free, it can be produced at a very small scale (down to hundreds of μm) without the need for extremely complex micromanipulation. Moreover, by attaching a small magnet to this mechanism and placing it over a rotating magnet we show the smooth movement of this structure. It is possible due to very fine gaps between different moving parts of the structure (less than 10 μm) and very good surface roughness (~200 nm RMS) possible due to optimisation presented previously in this article, which allows minimizing excessive friction. Pictures of Geneva mechanism movement are shown in Fig. 8(g). In the testing, it was shown that it can rotate up to 2000 RPM and that it can run for more than 100 hours continuously without any damage or other adverse impacts to the functionality. It is important to note that the measurement of Geneva mechanism rotation was carried out using simple rotating magnet underneath the

Optics EXPRESS

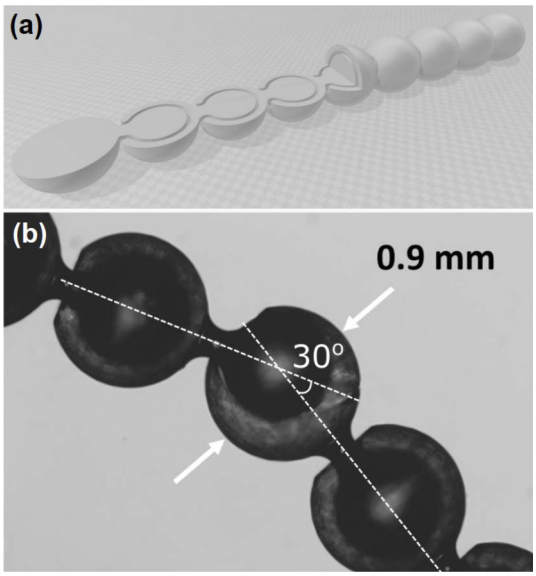

Fig. 7. Flexible chain with ball joints. (a) - 3D model of a structure, with 1/4 of the structure cut away to show hollow openings separating outer and inner balls in the joint. (b) optical microscope image of part of the structure. Bending at modeled 30^o is achieved. Also, inner and outer balls in the joint are clearly visible.

structure itself. As it was proof of concept experiment, our goal was to see if the mechanism would rotate without any trouble. Thus, the upper limit of the experiment was determined not by the structure, but by the measurement equipment. We estimate that at particularly high rotation speeds fragile mechanism axis would not be able to hold the rotation of the whole mechanism and break. However, we did not manage to reach such RPM in this work, leaving this investigation for future research.

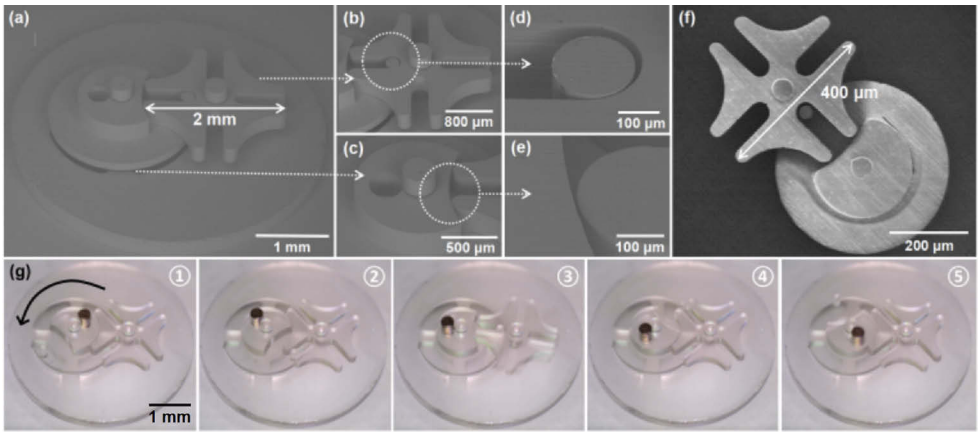

Fig. 8. Pictures of produced Geneva mechanism: (a) scanning electron microscope (SEM) image of the whole mechanism, (b)-(e) SEM pictures of the most important features and surfaces of the mechanism, and (f) SEM image of 5 times smaller Geneva mechanism than in part (a). (g) - Chronological pictures of Geneva mechanism movement, black arrow indicates the rotation direction. Magnet is attached to the structure the whole mechanism is inserted into a changing magnetic field for the movement automation.

Optics EXPRESS

The scalability of SLE should also be commended. As such structures will most likely find it's way to being used in high-precision complex devices, the possibility to easily tune the size and shape of structures towards mass customization is one of the top priorities. To demonstrate that SLE complies with such requirement we made a Geneva mechanism which is 5 times smaller than the original one [Fig. 8(f)]. Of course, some peculiarities exist in such a scale. The most important role in this process is played by the phenomena of selectivity. As a result, reducing the size of a structure is relatively easier than making it bigger. To avoid over-etching of unexposed parts of the structure, the etching rate should be sufficient if bigger structures are needed. An increase in selectivity has a fundamental limit, bounding complex SLE 3D fabrication to structures that are below several cm. Nevertheless, this is not a hard limit, if some compromises can be made to the structure accuracy, as the main hindrance of long etching times is an excessive dissolving of laser unaffected glass volume. If some taper can be tolerated, even cm-sized structures can be produced using SLE.

4. Discussion

The field of micro-robotics and micromechanics is extremely active [41,42]. Multitude of deformable [43,44], intertwined [32,45] or assembled [46] structures were presented over the years. However, most of them are produced either from polymers, metals, or some composite containing both. Glass, on the other hand, is highly underutilized in this field. In this work, we showed that glass can be exploited in the field of micromechanics a lot more, opening the door for was array of novel structures which were never tried before at this scale, like Geneva mechanism or related multi-component structures. Indeed, the mechanical properties of glass are very well known, repeatable, and not dependent on the SLE process itself. This is in sharp contrast to polymers, which, when microstructured with fs-laser in 3D present a multitude of degrees of freedom in terms of mechanical and optical properties. These depend on cross-linking [47] degree and even on surrounding medium [48]. Additionally, even the most resilient polymers can withstand only temperatures up to several hundred degrees [49], while the melting point of fused silica is around 1500^{o}C. Therefore, glass offers a substantially better alternative to many currently popular materials in micro-robotics if the application in question requires the constant presence of organic solvents, high temperatures, or is otherwise hazardous and can cause polymers to degrade.

At the same time, SLE should not be entirely considered as a possible alternative for additive manufacturing *via* 3DLL. These two methodologies can supplement each other as well. It was already showed that using chemically inert SLE etched cantilever and integrated polymer rod a passive actuator, which moves in accordance to the organic solvent present in the system, might be created [38]. Some micromechanical elements were fabricated in our work are smaller than what has been shown in the literature so far, allowing us to think about even more exotic applications. For instance, glass and polymer might be used in tandem to create polymer-glass structures, resembling already shown bi-polymer elements [50]. Alternatively, SLE, which is very efficient in fabricating microchannels, can be used for lab-on-chip system manufacturing, while 3DLL can provide integrated elements, like a filter, with a lot smaller features than SLE allows [51]. Such mix and matching of technologies are made even more attractive by the possibility to realize it using just a single amplified fs laser source integrated into a highly customizable fabrication setup [15]. Therefore, the work presented here gives a comprehensive look at what structures can be produced using SLE and what are the process peculiarities and ways to optimize it for the best possible result.

5. Author contributions

A. Butkutė planned and performed all the experiments, analyzed results. T. Baravykas prepared all the 3D structures designs, CAD models, and fabrication algorithms. A. Butkutė, J. Stančikas,

Optics EXPRESS

and T. Tičkūnas fabricated and characterized 3D structures. R. Vargalis, L. Jonušauskas and T. Tičkūnas made SEM images. A. Butkutė and L. Jonušauskas have written the manuscript. V. Sirutkaitis, D. Paipulas, L. Jonušauskas and T. Tičkūnas provided general consulting about the topic and manuscript preparation. All authors reviewed the manuscript and gave improvement advises.

Funding. European Regional Development Fund (project 01.2.2-LMT-K-718-03-0029) with the Research Council of Lithuania.

Disclosures. The authors declare no conflicts of interest.

Data availability. Data underlying the results presented in this paper are not publicly available at this time but may be obtained from the authors upon reasonable request.

References

1. S. LoTurco, R. Osellame, R. Ramponi, and K. C. Vishnubhatla, "Hybrid chemical etching of femtosecond laser irradiated structures for engineered microfluidic devices," J. Micromech. Microeng. **23**(8), 085002 (2013).
2. J. Gottmann, M. Hermans, N. Repiev, and J. Ortmann, "Selective laser-induced etching of 3D precision quartz glass components for microfluidic applications-up-scaling of complexity and speed," Micromachines **8**(4), 110 (2017).
3. S. Kim, J. Kim, Y.-H. Joung, S. Ahn, J. Choi, and C. Koo, "Optimization of selective laser-induced etching (SLE) for fabrication of 3D glass microfluidic device with multi-layer micro channels," Micro Nano Sys. Lett. **7**(1), 15 (2019).
4. Y. Bellouard, "Shape memory alloys for microsystems: A review from a material research perspective," Mater. Sci. Eng., A **481-482**, 582–589 (2008).
5. J. Gottmann, M. Hermans, and J. ortmann, "Microcutting and hollow 3D microstructures in glasses by in-volume selective laser-induced etching (ISLE)," J. Laser Micro/Nanoeng. **8**(1), 15–18 (2013).
6. Y. Hu, S. Rao, S. Wu, P. Wei, W. Qiu, D. Wu, B. Xu, J. Ni, L. Yang, J. Li, J. Chu, and K. Sugioka, "All-glass 3D optofluidic microchip with built-in tunable microlens fabricated by femtosecond laser-assisted etching," Adv. Opt. Mater. **6**(9), 1701299 (2018).
7. S. Butkus, D. Paipulas, D. Kaškelyte, E. Gaižauskas, and V. Sirutkaitis, "Improvement of cut quality in rapid-cutting of glass method via femtosecond laser filamentation," J. Laser Micro/Nanoeng. **10**(1), 59–63 (2015).
8. P. von Witzendorff, L. Pohl, O. Suttmann, P. Heinrich, A. Heinrich, J. Zander, H. Bragard, and S. Kaierle, "Additive manufacturing of glass: CO2-laser glass deposition printing," Proc. CIRP **74**, 272–275 (2018).
9. R. M. Zaki, C. Strutynski, S. Kaser, D. Bernard, G. Hauss, M. Faessel, J. Sabatier, L. Canioni, Y. Messaddeq, S. Danto, and T. Cardinal, "Direct 3D-printing of phosphate glass by fused deposition modeling," Mater. Des. **194**, 108957 (2020).
10. F. Kotz, K. Arnold, W. Bauer, D. Schild, N. Keller, K. Sachsenheimer, T. M. Nargang, C. Richter, D. Helmer, and B. E. Rapp, "Three-dimensional printing of transparent fused silica glass," Nature **544**(7650), 337–339 (2017).
11. G. Merkininkaitė, D. Gailevičius, S. Šakirzanovas, and L. Jonušauskas, "Polymers for regenerative medicine structures made via multiphoton 3D lithography," Int. J. Polym. Sci. **2019**, 1–23 (2019).
12. F. Kotz, A. S. Quick, P. Risch, T. Martin, T. Hoose, M. Thiel, D. Helmer, and B. E. Rapp, "Two-photon polymerization of nanocomposites for the fabrication of transparent fused silica glass microstructures," Adv. Mater. **33**(9), 2006341 (2021).
13. A. Marcinkevičius, S. Juodkazis, M. Watanabe, M. Miwa, S. Matsuo, H. Misawa, and J. Nishii, "Femtosecond laser-assisted three-dimensional microfabrication in silica," Opt. Lett. **26**(5), 277–279 (2001).
14. A. Butkutė and L. Jonušauskas, "3D manufacturing of glass microstructures using femtosecond laser," Micromachines **12**(5), 499 (2021).
15. L. Jonušauskas, D. Mackevičiūtė, G. Kontenis, and V. Purlys, "Femtosecond lasers: the ultimate tool for high-precision 3D manufacturing," Adv. Opt. Technol. **8**(3-4), 241–251 (2019).
16. C. Hnatovsky, R. S. Taylor, E. Simova, V. R. Bhardwaj, D. M. Rayner, and P. B. Corkum, "Polarization-selective etching in femtosecond laser-assisted microfluidic channel fabrication in fused silica," Opt. Lett. **30**(14), 1867–1869 (2005).
17. C. A. Ross, D. G. Maclachan, D. Choudrury, and R. R. Thomson, "Optimisation of ultrafast laser assisted etching in fused silica," Opt. Express **26**(19), 24343–24356 (2018).
18. P. Paiè, F. Bragheri, D. D. Carlo, and R. Osellame, "Particle focusing by 3D inertial microfluidics," Microsyst. Nanoeng. **3**(1), 17027 (2017).
19. C. Hnatovsky, R. S. Taylor, E. Simova, P. P. Rajeev, D. M. Rayner, V. Bhardwaj, and P. B. Corkum, "Fabrication of microchannels in glass using focused femtosecond laser radiationand selectivechemical etching," Appl. Phys. A **84**(1-2), 47–61 (2006).
20. S. Matsuo, H. Sumi, S. Kiyama, T. Tomita, and S. Hashimoto, "Femtosecond laser-assisted etching of pyrex glass with aqueous solution of KOH," Appl. Surf. Sci. **255**(24), 9758–9760 (2009).
21. S. Juodkazis, Y. Nishi, and H. Misawa, "Femtosecond laser-assisted formation of channels in sapphire using KOH solution," Phys. Status Solidi RRL **2**(6), 275–277 (2008).
22. M. Hörstmann-Jungemann, J. Gottmann, and M. Keggenhoff, "3D-microstructuring of sapphire using fs-laser irradiation and selective etching," J. Laser Micro/Nanoeng. **5**(2), 145–149 (2010).

Optics EXPRESS

23. L. Capuanoa, R. Tiggelaar, J. Berenschot, J. Gardeniers, and G. Römer, "Fabrication of millimeter-long structures in sapphire using femtosecond infrared laser pulses and selective etching," Opt. Laser Eng. **133**, 106114 (2020).
24. A. Rodenas, M. Gu, G. Corrielli, P. Paie, S. John, A. K. Kar, and R. Osellame, "Three-dimensional femtosecond laser nanolithography of crystals," Nat. Photonics **13**(2), 105–109 (2019).
25. J. Hua, H. Ren, A. Jia, Z. Tian, L. Wang, S. Juodkazis, Q. Chen, and H. Sun, "Convex silica microlens arrays via femtosecond laser writing," Opt. Lett. **45**(3), 636–639 (2020).
26. Y. Lu, X. Liu, L. Zhu, Q. Chen, S. Juodkazis, and H. Sun, "Vector scanning subtractive manufacturing technology for laser rapid fabrication," Opt. Lett. **46**(8), 1963–1966 (2021).
27. S. Butkus, M. Rickus, R. Sirutkaitis, D. Paipulas, and V. Sirutkaitis, "Fabrication of high aspect ratio channels in fused silica using femtosecond pulses and chemical etching at different conditions," J. Laser Micro/Nanoeng. **14**(1), 19–24 (2019).
28. S. Juodkazis, K. Yamasaki, V. Mizeikis, S. Matsuo, and H. Misawa, "Formation of embedded patterns in glasses using femtosecond irradiation," Appl. Phys. A **79**(4-6), 1549–1553 (2004).
29. M. Hermans, J. Gottmann, and F. Riedel, "Selective, laser-induced etching of fused silica at high scan-speeds using koh," J. Laser Micro/Nanoeng. **9**(2), 126–131 (2014).
30. X. Li, J. Xu, Z. Lin, J. Qi, P. Wang, W. Chu, Z. Fang, Z. Wang, Z. Chai, and Y. Cheng, "Polarization-insensitive space-selective etching in fused silica induced by picosecond laser irradiation," Appl. Surf. Sci. **485**, 188–193 (2019).
31. J. Qi, Z. Wang, J. Xu, Z. Lin, X. Li, W. Chu, and Y. Cheng, "Femtosecond laser induced selective etching in fused silica: optimization of the inscription conditions with a high-repetition-rate laser source," Opt. Express **26**(23), 29669–29678 (2018).
32. L. Jonušauskas, T. Baravykas, D. Andrijec, T. Gadišauskas, and V. Purlys, "Stitchless support-free 3D printing of free-form micromechanical structures with feature size on-demand," Sci. Rep. **9**(1), 17533 (2019).
33. S. K. Sundaram and E. Mazur, "Inducing and probing non-thermal transitions in semiconductors using femtosecond laser pulses," Nat. Mater. **1**(4), 217–224 (2002).
34. R. S. Taylor, C. Hnatovsky, E. Simova, P. P. Rajeev, D. M. Rayner, and P. B. Corkum, "Femtosecond laser erasing and rewriting of self-organized planar nanocracks in fused silica glass," Opt. Lett. **32**(19), 2888–2890 (2007).
35. L. Jonušauskas, D. Gailevičius, S. Rekštytė, T. Baldacchini, S. Juodkazis, and M. Malinauskas, "Mesoscale laser 3D printing," Opt. Express **27**(11), 15205–15221 (2019).
36. Y. Xia and G. M. Whitesides, "Soft lithography," Annu. Rev. Mater. Sci. **28**(1), 153–184 (1998).
37. L. Jonušauskas, S. Rekštytė, R. Buividas, S. Butkus, R. Gadonas, S. Juodkazis, and M. Malinauskas, "Hybrid subtractive-additive-welding microfabrication for lab-on-chip (LOC) applications via single amplified femtosecond laser source," Opt. Eng. **56**(9), 094108 (2017).
38. T. Tičkūnas, M. Perrenoud, S. Butkus, R. Gadonas, S. Rekštytė, M. Malinauskas, D. Paipulas, Y. Bellouard, and V. Sirutkaitis, "Combination of additive and subtractive laser 3D microprocessing in hybrid glass/polymer microsystems for chemical sensing applications," Opt. Express **25**(21), 26280–26288 (2017).
39. N. Noeth, S. S. Keller, and A. Boisen, "Integrated cantilever-based flow sensors with tunable sensitivity for in-line monitoring of flow fluctuations in microfluidic systems," Sensors **14**(1), 229–244 (2013).
40. Y. Bellouard, R. Clavel, J.-E. Bidaux, R. Gotthardt, and T. Sidler, "A concept for monolithic shape memory alloys micro-devices," J. Phys. IV **07**(C5), C5-603–C5-608 (1997).
41. S. Koo, "Advanced micro-actuator/robot fabrication using ultrafast laser direct writing and its remote control," Appl. Sci. **10**(23), 8563 (2020).
42. A.-I. Bunea, D. Martella, S. Nocentini, C. Parmeggiani, R. Taboryski, and D. S. Wiersma, "Light-powered microrobots: Challenges and opportunities for hard and soft responsive microswimmers," Adv. Intell. Syst. **3**(4), 2000256 (2021).
43. R. Suriano, T. Zandrini, C. de Marco, R. Osellame, S. Turri, and F. Bragheri, "Nanomechanical probing of soft matter through hydrophobic AFM tips fabricated by two-photon polymerization," Nanotechnology **27**(15), 155702 (2016).
44. I. Spanos, Z. Vangelatos, C. Grigoropoulos, and M. Farsari, "Design and characterization of microscale auxetic and anisotropic structures fabricated by multiphoton lithography," Nanomaterials **11**(2), 446 (2021).
45. M. Power, A. J. Thompson, S. Anastasova, and G.-Z. Yang, "A monolithic force-sensitive 3D microgripper fabricated on the tip of an optical fiber using 2-photon polymerization," Small **14**(16), 1703964 (2018).
46. J. Kohler, S. I. Ksouri, C. Esen, and A. Ostendorf, "Optical screw-wrench for microassembly," Microsyst. Nanoeng. **3**(1), 16083 (2017).
47. L. Pertoldi, V. Zega, C. Comi, and R. Osellame, "Dynamic mechanical characterization of two-photon-polymerized SZ2080 photoresist," J. Appl. Phys. **128**(17), 175102 (2020).
48. S. Rekštytė, D. Paipulas, M. Malinauskas, and V. Mizeikis, "Microactuation and sensing using reversible deformations of laser-written polymeric structures," Nanotechnology **28**(12), 124001 (2017).
49. L. Jonušauskas, D. Gailevičius, L. Mikoliūnaitė, D. Sakalauskas, S. Šakirzanovas, S. Juodkazis, and M. Malinauskas, "Optically clear and resilient free-form μ-optics 3D-printed via ultrafast laser lithography," Materials **10**(1), 12 (2017).
50. J. Qu, M. Kadic, A. Naber, and M. Wegener, "Micro-structured two-component 3D metamaterials with negative thermal-expansion coefficient from positive constituents," Sci. Rep. **7**(1), 40643 (2017).
51. D. Wu, S.-Z. Wu, J. Xu, L.-G. Niu, K. Midorikawa, and K. Sugioka, "Hybrid femtosecond laser microfabrication to achieve true 3D glass/polymer composite biochips with multiscale features and high performance: the concept of ship-in-a-bottle biochip," Laser Photonics Rev. **8**(3), 458–467 (2014).